Published in final edited form as:
Cell. 2007 January 26; 128(2): 309–323.

FoxOs are lineage-restricted redundant tumor suppressors and critical regulators of endothelial cell homeostasis

Ji-Hye Paik[1,*], **Ramya Kollipara**[1,*], **Gerald Chu**[1,2,3], **Hongkai Ji**[4], **Yonghong Xiao**[3], **Zhihu Ding**[1], **Lili Miao**[1,3], **Zuzana Tothova**[5], **James W. Horner**[1], **Daniel R. Carrasco**[1,3], **Shan Jiang**[1], **D. Gary Gilliland**[5], **Lynda Chin**[1,3,6], **Wing H. Wong**[7], **Diego H. Castrillon**[1,8], and **Ronald A. DePinho**[1,3]

1 *Department of Medical Oncology, Dana-Farber Cancer Institute, and Departments of Medicine and Genetics, Harvard Medical School, Boston, MA 02115, USA*

2 *Department of Pathology, Brigham and Women's Hospital, Harvard Medical School, Boston, MA 02115, USA*

3 *Center for Applied Cancer Science, Belfer Foundation Institute for Innovative Cancer Science, Dana-Farber Cancer Institute, Harvard Medical School, Boston, MA 02115, USA*

4 *Department of Statistics, Harvard University, Cambridge, MA 02138, USA*

5 *Division of Hematology, Department of Medicine, Brigham and Women's Hospital, Boston, MA 02115, USA*

6 *Department of Dermatology, Harvard Medical School, Boston, MA 02115, USA*

7 *Department of Statistics, Stanford University, Stanford, CA 94305, USA*

8 *Department of Pathology and Simmons Comprehensive Cancer Center, University of Texas Southwestern Medical School, Dallas, TX 75390, USA*

Abstract

Activated phosphoinositide 3-kinase (PI3K)-AKT signalling appears to be an obligate event in the development of cancer. The highly related members of the mammalian FoxO transcription factor family, FoxO1, FoxO3 and FoxO4, represent one of several effector arms of PI3K-AKT signalling, prompting genetic analysis of the role of FoxOs in the neoplastic phenotypes linked to PI3K-AKT activation. While germline or somatic deletion of up to 5 FoxO alleles produced remarkably modest neoplastic phenotypes, broad somatic deletion of all FoxOs engendered a progressive cancer-prone condition characterized by thymic lymphomas and hemangiomas, demonstrating that the mammalian FoxOs are indeed bona fide tumor suppressors. Transcriptome and promoter analyses of differentially affected endothelium identified novel direct FoxO targets and revealed that FoxO regulation of these targets in vivo is highly context-specific, even in the same cell type. Functional studies validated Sprouty2 and PBX1, among others, as FoxO-regulated mediators of endothelial cell morphogenesis and vascular homeostasis.

Author Information. The authors declare no competing financial interests. Correspondence should be addressed to D.H.C. (diego.castrillon@utsouthwestern.edu) and R.A.D. (ron_depinho@dfci.harvard.edu)..
*These authors contributed equally to this work.

Introduction

The PI3K-AKT pathway is activated in human cancers, commonly through genetic alterations of its many signalling components. AKT and the p110α catalytic subunit of PI3K is mutated or amplified and overexpressed in several cancer types, and PTEN, the key PI3K-AKT pathway antagonist, is also inactivated in a broad spectrum of human cancers (Cully et al., 2006). Moreover, germline PTEN mutations define three related syndromes characterized by hamartomas, cancer and developmental defects (Wanner et al., 2001). PTEN's diverse tumor suppressor role in different cell lineages is further evidenced by the cancer-prone condition in germline and conditional *Pten* mutant mice, which develop carcinomas of the skin, prostate, colon, breast, and endometrium, as well as thymic lymphomas, among other cancers (Di Cristofano et al., 1998; Li et al., 2002; Podsypanina et al., 1999; Suzuki et al., 2001; Wang et al., 2003; You et al., 2002). In addition to a direct role in tumor development, PI3K-AKT signalling has been linked to endothelial cell homeostasis (Shiojima and Walsh, 2002). One of the PTEN germline mutation syndromes, Bannayan-Zonana, is characterized by hemangiomas (endothelial cell hamartomas) in diverse tissues (Wanner et al., 2001), and *Pten* heterozygous mice develop hemangiomas with high penetrance (Freeman et al., 2006).

The wide range of benign to malignant phenotypes mediated by PI3K-PTEN-AKT signalling is consistent with the existence of diverse downstream effectors differentially utilized in conferring neoplastic phenotypes in distinct cell lineages. Among such potential effectors are AKT phosphorylation targets TSC2, GSK3 and the FoxOs (Brunet et al., 1999; Cross et al., 1995; Inoki et al., 2002). Recently, much attention has been focused on TSC2 and mTOR signalling as mounting pharmacological evidence suggests that mTOR is the prime effector of the PI3K-AKT pathway, with TSC2 serving as a central node linking LKB1-AMPK and PI3K-AKT with mTOR (Hay, 2005). Indeed, the potent anti-neoplastic impact of pharmacologic mTOR inhibition raises questions as to the relevance of other AKT targets, particularly the FoxOs, in the development of cancer. On the other hand, the FoxO effector arm controls cell number in Drosophila (Junger et al., 2003; Puig et al., 2003), and the FoxO transcription factors mediate some of the growth and survival-promoting effects of AKT signaling in endothelial cells (Potente et al., 2005; Skurk et al., 2004). Therefore, the relevance of FoxO transcription factors in cancer and their roles in normal tissue homeostasis remain to be elucidated.

Whereas *C. elegans* and *D. melanogaster* contain a single *FoxO* gene (DAF-16 and dFOXO, respectively), mice and humans possess three highly related *FoxO* homologues (*FoxO1*, *FoxO3*, and *FoxO4*) with overlapping patterns of expression and transcriptional activities (Anderson et al., 1998; Biggs et al., 2001; Furuyama et al., 2000). A fourth more distantly related mammalian FoxO family member, *FoxO6*, has been identified, although it appears to be regulated by distinct mechanisms and its expression is more highly restricted to the brain (Jacobs et al., 2003; van der Heide et al., 2005).

In cell culture-based systems, FoxO1, FoxO3, and FoxO4 behave similarly in biochemical studies, appear to regulate common target genes, and bind to the same target DNA sequence (Biggs et al., 2001; Brunet et al., 1999; Furuyama et al., 2000). Yet, mouse *FoxO* knockouts have revealed unique roles for the FoxOs, such as the requirement for FoxO3 in ovarian primordial follicle activation (Castrillon et al., 2003; Hosaka et al., 2004) and for FoxO1 in vasculogenesis (Furuyama et al., 2004; Hosaka et al., 2004). However, while the three FoxOs serve some discrete functions, they likely have significant redundancies, as they are broadly expressed during embryonic and adult tissues (Furuyama et al., 2000). In this regard, conventional genetic analysis can fail to uncover important biological functions among closely-related gene families, such as Rb/p107/p130 (Lee et al., 1996; Sage et al., 2000) and p53/p63/p73 (Flores et al., 2005; Flores et al., 2002). Indeed, many analogies can be drawn between the

FoxO, Rb, and p53 gene families, all of which regulate cell survival and growth and consist of members with common physiological roles.

In the context of the linkage of FoxOs to key cancer signaling pathways, the lack of an overt tumor-prone phenotype of the various FoxO knockout mice was somewhat unanticipated (Castrillon et al., 2003; Hosaka et al., 2004; Lin et al., 2004). While this may relate to the physical and functional relatedness and overlapping expression patterns of the FoxO members, it is formally possible that the FoxO arm of the PI3K-AKT signaling network plays a relatively minor *in vivo* role in cancer suppression and vascular biology relative to other AKT downstream targets. To address these issues, we have generated conditional alleles for all three FoxO members with which to conduct a systematic evaluation of FoxO family function *in vivo*.

Results

Somatic deletion of all three FoxO genes results in lineage-restricted tumor phenotypes

To genetically assess the cancer relevance of the FoxO members *in vivo*, we generated null and conditional alleles for all three *FoxO* genes (Supplemental text and Figures S1, S2). Exhaustive characterization of mice bearing single and compound germline *FoxO* null mutations, including $FoxO1^{-/+}$; $FoxO3^{-/-}$; $FoxO4^{-/-}$ mice revealed remarkably mild cancer predisposition phenotypes as a function of advancing age or following carcinogen treatment (Figures S3-S6, Table S1). The potential for redundancy and developmental compensation among the FoxOs, coupled with the embryonic lethality of FoxO1 deficiency (Furuyama et al., 2004; Hosaka et al., 2004), prompted the use of the inducible *Mx-Cre* transgene to achieve widespread somatic FoxO deletion in adult tissues. The *Mx1* promoter is activated by polyinosine-polycytidylic acid (pI-pC), and pI-pC injection at 4–5 weeks of age results in transient widespread Cre expression (Kuhn et al., 1995) (see *Mx1 promoter*-directed tissue distribution of Cre below).

To delete the *FoxO* genes *in vivo*, $Mx\text{-}Cre^{+}$;$FoxO1/3/4^{L/L}$ and control littermate $Mx\text{-}Cre^{-}$;$FoxO1/3/4^{L/L}$ mice (hereafter designated as "$Mx\text{-}Cre^{+}$" and "$Mx\text{-}Cre^{-}$ ", respectively) were injected with pI-pC. By 19–30 weeks of age, $Mx\text{-}Cre^{+}$ mice developed aggressive $CD4^{+}$ $CD8^{+}$ lymphoblastic thymic lymphomas, with spread to spleen, liver, and lymph nodes (Figure 1a, b, and f, $p<0.0001$). While *Mx-Cre*-mediated gene deletion in the thymus was incomplete (Kuhn et al., 1995) (Figure 1c), the lymphomas display an enrichment of the null alleles for all three *FoxO* genes (Figure 1c) accompanied by a marked decrease of FoxO expression on both mRNA and protein levels (Figure 1d and e). This and the lack of lymphomas in all other genotypes retaining at least one *FoxO* allele (Figure 1a) is consistent with the need for complete FoxO deficiency in lymphomagenesis.

In addition, all $Mx\text{-}Cre^{+}$ mice developed a striking age-progressive hamartomatous phenotype in the endothelial cell lineage, with widespread hemangiomas, resulting in premature death (Figure 2a). Hemangiomas were most exaggerated in the uterus and evident by 6–8 weeks, but greatly progressed by 30–40 weeks (Figure 2b). Histological examination revealed massive hemangiomas with intraluminal blood and thrombi in skeletal muscle, abdominal wall, liver, adrenal glands, bone marrow, omentum, lymph node, and skin (Figure 2c; Supplemental Figure S7a). The endothelial cells in most lesions appeared benign; however, 9% of $Mx\text{-}Cre^{+}$ mice progressed to lethal angiosarcomas (Figure 2c).

Labelling of endothelial cells with fluorescein-conjugated lectin revealed significant increases in the number of endothelial cells in affected organs (Figure 2d). This proliferative phenotype was apparent as early as three weeks after pI-pC injection, prior to onset of macroscopic abnormalities in these vascular beds. In contrast, endothelial cells in the lung and kidney (where hemangiomas do not develop following documented *FoxO* deletion) did not show any

abnormalities even at 27 weeks after pI-pC injection, establishing tissue-context requirements for the FoxOs *in vivo* across this single lineage (Figure 2d).

Further support for a role of the FoxOs in this vascular phenotype stems from observations of less severe hemangiomas in *Mx-Cre*$^{+}$ mice with deficiency of only one or two *FoxO* genes. By 60 weeks of age, 100% of *Mx-Cre*$^{+}$*;FoxO1*$^{L/L}$ females displayed mild hemangiomas in the uterus and occasionally in perirenal fat, with no abnormalities in other tissues (Supplemental Figure S7b). *Mx-Cre*$^{+}$*;FoxO1/4*$^{L/L}$ mice also displayed mild hemangiomas in the uterus and occasionally in other tissues (Supplemental Figure S7c), and all *Mx-Cre*$^{+}$*;FoxO1/3* $^{L/L}$ mice displayed vascular abnormalities with similar tissue distribution as *Mx-Cre*$^{+}$*;FoxO1/3/4*$^{L/L}$ mice (Supplemental Figure S7d). Importantly, these hemangiomatous lesions retaining either FoxO3 or FoxO4 were significantly less severe as reflected by lack of mortality prior to 50 weeks of age (Figure 2a). In contrast, vascular abnormalities were not detected in *Mx-Cre*$^{+}$*;FoxO3*$^{L/L}$ mice up to 21 weeks and in germline *FoxO3*$^{-/-}$; *FoxO4*$^{-/-}$ mice up to 2 years of age and *FoxO1*$^{-/+}$*; FoxO3*$^{-/-}$*; FoxO4*$^{-/-}$ mice up to 40 weeks of age. These genotype-phenotype correlations point to FoxO1 as the most potent regulator of adult vascular homeostasis, with lesser but physiologically important contributions from the other FoxOs. In summary, vascular lesions were much more pervasive and severe following elimination of all three FoxOs, and premature mortality attributable to these vascular lesions was observed only in mice with somatic deletion of all three FoxOs (Figure 2a).

Cell biological impact of FoxO family deletion

To understand how the FoxOs constrain the development of thymic lymphoma and hemangiomas, we examined the proliferative and survival profiles of thymocyte and endothelial cells derived from young cancer-free mice. Although histologically normal (data not shown) albeit with a slight reduction in total number of thymocytes compared to *Mx-Cre*$^{-}$controls (99,110,000 ± 13,590,000 versus 147,300,000 ± 20,950,000; n=6 each; p=0.0825), *Mx-Cre*$^{+}$ thymocytes exhibited altered responses to growth and death stimuli. Upon stimulation with PMA + ionomycin, *Mx-Cre*$^{+}$ thymocytes showed increased proliferation relative to *Mx-Cre*$^{-}$ controls (Figure 3a). Proliferative enhancement was also observed with CD3 + IL2 stimulation (Figure 3a). Conversely, *Mx-Cre*$^{+}$ thymocytes were more resistant to cell death stimuli such as γ-irradiation and high-dose dexamethasome treatment (Figure 3a). These observations indicate that complete loss of *FoxO* gene function in thymocytes predisposes to lymphomagenesis through cell autonomous mechanisms that enhance cellular proliferation and survival.

Taking advantage of efficient *Mx-Cre* mediated recombination in endothelial cells (ECs) in all tissue compartments examined (Supplemental Figure S8) (Hayashi et al., 2004; Schneider et al., 2003) and the organ-restricted hemangioma phenotype in *Mx-Cre*$^{+}$ mice, we compared the biological consequences of complete *FoxO* deletion in ECs from affected and unaffected vascular beds in different tissues. ECs were isolated and cultured from lung (which displayed no phenotype *in vivo*) and liver (which displayed prominent hemangiomatous changes) from age-matched mice. The purity of these cell preparations was >97% by flow cytometry for CD31 and immunostaining for VE-cadherin and CD31 (Supplemental Figure S9a,b). Efficient deletion of all three *FoxO* alleles was confirmed by PCR, and western blot documented absence of FoxO protein in both lung and liver ECs (Supplemental Figure S9c,d). In vivo, absence of mRNA for all three FoxOs in the vasculature of lung, liver, and uterus was documented by RNA *in situ* hybridization (RISH) (Supplemental Figure S10).

Relative to *Mx-Cre*$^{+}$ lung ECs, *Mx-Cre*$^{+}$ liver ECs showed enhanced proliferative response to stimulation by VEGF and bFGF, two potent pro-angiogenic cytokines (Bikfalvi et al., 1997; Ferrara et al., 2003). While *Mx-Cre*$^{-}$ and *Mx-Cre*$^{+}$ lung ECs responded to VEGF similarly regardless of their FoxO status, *Mx-Cre*$^{+}$ liver ECs exhibited a dramatic enhancement in their

ability to proliferate upon VEGF stimulation (Figure 3b; 73% vs. 17.9%, p=0.003). A similar trend was observed with bFGF stimulation (p=0.019; data not shown). Conversely, *Mx-Cre*$^{+}$ liver ECs were significantly less sensitive to TGF-β1, a cytokine that induces EC cytostasis through Smad (Goumans et al., 2003), consistent with documented direct interactions between Smad and FoxO (Seoane et al., 2004). Here, *Mx-Cre*$^{-}$liver ECs showed reduced survival (~60%) upon exposure to TGF-β1, whereas *Mx-Cre*$^{+}$ liver ECs were much less sensitive (Figure 3b). Interestingly, lung ECs were insensitive to TGF-β1 stimulation irrespective of FoxO status (Figure 3b). In summary, mirroring the *in vivo* phenotypes, FoxO-deficient liver ECs exhibited enhanced proliferative and survival potential, while FoxO-deficient lung ECs did not show detectable phenotypic alterations. That FoxO exerts these biological effects in a cell autonomous manner is supported by the observation of a prominent hemangiomatous phenotype in skeletal muscle, which showed a lack of *Mx-Cre*-mediated recombination in the surrounding skeletal muscle fibers yet efficient recombination in the endothelium (Supplemental Figure S8k).

Integrated transcriptome and promoter analysis identifies novel direct FoxO targets in vivo

The above *in vivo* and *in vitro* phenotypic characterization shows that FoxO family functions in normal tissue homeostasis and in cancer suppression are not only lineage-restricted, but also organ-specific. To gain additional insights into the mechanistic basis for such specificity, we conducted comparative transcriptome analyses of purified lung and liver ECs following pI-pC treatment of age-matched *Mx-Cre*$^{+}$ and *Mx-Cre*$^{-}$ mice. We hypothesized that normalization against phenotypically unaffected lung ECs would provide an effective biological filter for identifying physiologically relevant FoxO targets versus secondary/bystander transcriptional events – the latter would include genes whose expression responds to FoxO regulation but do not play a rate-limiting role in the observed phenotypes as well as those whose expression might be altered by activation of Cre expression during FoxO deletion. Transcriptome profiles of liver ECs with and without functional FoxOs were compared with those of lung ECs (see Methods) to generate a list of 138 significantly differentially expressed genes - 89 of which were upregulated and 49 downregulated in liver but not in lung ECs upon documented FoxO deletion (Supplemental Table S3). Consistent with the observed *in vivo* phenotypes, several differentially expressed genes have validated roles in EC biology, angiogenesis and tissue morphogenesis, such as XLKD1 (LYVE-1), VCAM1, angiopoietin-like 4 (ANGPTL4), adrenomedullin (ADM), thrombospondin1 (THBS1), and ID1, and extracellular matrix proteins such as fibrillin (FBN1) (Benezra, 2001; Cook-Mills, 2002; Kato et al., 2005; Le Jan et al., 2003; Mouta Carreira et al., 2001; Ramirez et al., 1993).

Next, we reasoned that the identification of FoxO binding elements (BEs) in differentially expressed genes would provide more direct insights into FoxO's actions in the observed phenotypes. To that end, we conducted a systematic *in silico* analysis of the regulatory regions of these 138 genes to ascertain the presence of evolutionarily conserved FoxO consensus BEs. For each gene, the −8kb to +2kb region surrounding the transcription start site and the 0 to +5kb region downstream of the transcription end site in the mouse genome were surveyed. We constructed a position specific weight matrix (PWM) based on evolutionary conservation of canonical insulin-regulated FoxO targets (IGFBP1, G6PD, PEPCK) to characterize the FoxO binding motif (consensus = BBTRTTTTD) (D.H.C., unpublished data). Potential FoxO BEs were filtered further by cross-species conservation with two independent methodologies (Supplementary methods). BEs that could be identified in mouse, human and at least one other species were designated as a "3-species conserved" BE. By requiring at least one evolutionary conserved FoxO BEs predicted by both methods, we identified 21 putative direct targets of FoxO family in liver ECs, 9 of which were down-modulated and 12 up-modulated upon FoxO deletion (Table 1). Interestingly, several of these genes are highly relevant to cancer (e.g., TCF4), vascular biology (e.g., CTGF), or both, such as ID1 and ADM, two factors known to

play critical roles in EC survival and promote angiogenesis during development and tumorigenesis (Benezra, 2001;Kato et al., 2005;Nikitenko et al., 2006) (see discussion).

To validate our computational approach, we sought to document direct binding of FoxOs on predicted BEs by ChIP (chromatin immunoprecipitation) and confirm expression modulation by RT-qPCR and RNA in situ hybridization (RISH) *in vitro* and *in vivo*, respectively (Table 1). Figure 4 illustrates the validation of *Sprouty2* as a direct FoxO target. First, using a mixture of anti-FoxO1/3/4 antibodies, DNA fragments spanning FoxO BEs from both the proximal and distal regions of *Sprouty2* gene were more efficiently co-immunoprecipitated in the FoxO-expressing liver ECs, versus those deficient for the FoxOs (Figure 4b). Next, we documented, by immunoblotting and quantitative RT-PCR, that *Sprouty2* was significantly and reproducibly downregulated in independently derived $MxCre^{+}$ liver ECs, but not in $MxCre^{+}$ lung ECs (Figure 4c, d). Mindful of the potential artefact introduced by culturing EC *in vitro*, we next performed RISH in tissue sections to confirm that *Sprouty2* mRNA levels were comparable in $MxCre^{-}$ and $MxCre^{+}$ lung EC but were significantly down-modulated in vascular beds of affected tissues including liver, skeletal muscle, and uterus in $Mx\text{-}Cre^{+}$ mice 3 weeks after treatment with pI-pC (Figure 4e).

For the other targets, we conducted similar validation studies. By RISH, 12 of 14 randomly selected putative targets exhibited transcriptional regulation by FoxO *in vivo* (Supplemental Figure S11). Of note, *Meis1* and *Klf6* which did not confirm by RISH, were shown to be regulated by RT-qPCR, pointing to the detection limits of RISH. Moreover, all 17 randomly selected putative targets (8 down-modulated and 9 up-modulated) showed expression modulation by RT-qPCR in response to FoxO deletion in culture (data not shown; Table 1). Finally, all 8 randomly selected putative targets (6 down-modulated and 2 up-modulated) were validated to be true direct targets of FoxO by ChIP (Supplemental Figure S12). Thus, 8 of 8 putative targets satisfied both ChIP and expression validation (Table 1), indicating the robustness of our integrated computational-biological approach in the identification of novel direct targets of FoxOs in ECs *in vivo*.

FoxO activities are lineage-restricted in vivo

Next, to address whether the spectrum of downstream effectors of the FoxOs are further dictated by cell type, we performed similar *in silico* promoter analysis on a list of 354 most differentially expressed genes in the thymocyte lineage (Supplemental Table S2) and compared these profiles with those in ECs. Strikingly, putative direct targets with predicted conserved FoxO BEs and transcriptionally regulated by FoxOs in thymocytes were completely non-overlapping with those in EC lineage (Table 2). A notable FoxO target in thymocytes is $p27^{KIP1}$ (*CDKN1B*), one of the downregulated genes with the highest conservation score and number of three-species BE's (see discussion). In other words, this *in silico* analysis not only identified putative targets of direct FoxO regulation, but also demonstrated in molecular terms that signalling downstream of FoxO is both cell type-specific and tissue-specific within the same cell type. These molecular findings provide mechanistic insights and a potential explanation for the more restricted phenotypic impact of FoxO deletion relative to activated PI3K-AKT signalling in various organ systems.

Direct effectors of FoxO-regulated endothelial cell homeostasis

To elucidate further the mechanistic basis of FoxO dysregulation in hemangioma development, we first focused on *Sprouty2* for biological validation, as it represented the most significantly regulated gene with highest number of conserved FoxO BEs in affected liver but not lung EC. Using two independent Sprouty2 shRNAs (shSPRY2-1 and shSPRY2-2), Sprouty2 protein knockdown of 73% to 75% was documented in primary cultures of liver ECs (Figure 5c). Passage-associated proliferative arrest of $Mx\text{-}Cre^{-}$ primary liver EC was reversed by Sprouty2

knockdown, conferring enhanced replicative potential to *Mx-Cre*$^{-}$ ECs similar to that of FoxO-deficient *Mx-Cre*$^{+}$ ECs (Figure 5a). Correspondingly, increased cell cycle progression and decreased apoptosis could be demonstrated upon Sprouty2 knockdown. Specifically, the BrdU positive population in *Mx-Cre*$^{-}$ liver EC cultures was increased with shSPRY2-1 and shSPRY2-2, comparable to the level of proliferation in *Mx-Cre*$^{+}$ liver ECs. Importantly, further reduction in Sprouty2 expression in *Mx-Cre*$^{+}$ liver ECs had no additional effects (Figure 5b). Similarly, TUNEL positivity in *Mx-Cre*$^{-}$ liver ECs decreased from 19% to 7% ($p<0.01$), comparable to the reduction to 5% observed in *Mx-Cre*$^{+}$ liver ECs ($p<0.01$). Associated with these phenotypic changes were differential expression of CyclinD1, p15, and p21 expression as well as Bim following Sprouty2 shRNA knockdown (Figure 5d), reinforcing the view that Sprouty2 functions as a negative regulator of EC proliferation and survival. Finally, in matrigel morphogenesis assays, *Mx-Cre*$^{+}$ liver ECs developed a more robust tube network compared to *Mx-Cre*$^{-}$ liver ECs (Figure 5e). Again, knockdown of Sprouty2 in *Mx-Cre*$^{-}$ liver ECs enhanced such VEGF-induced tube formation to levels approaching those of *Mx-Cre*$^{+}$ liver ECs (Figure 5e). Taken together, these results demonstrate that Sprouty2 plays essential roles in EC growth and tube morphogenesis and is a major effector of FoxO function in the endothelium.

To assess additional contributions from other validated or putative direct FoxO targets listed in Table 1, knockdown studies were conducted on an additional set of FoxO-upregulated genes (ADM, CTGF, MRC1, and CCRN4L); and FoxO-down-regulated genes (PBX1, ID1, and BMPER). These assays revealed that PBX1 exhibited robust activities in both EC proliferation and apoptosis assays similar to Sprouty2 and two targets (CTGF and ADM) showed modest effects on EC growth but not apoptosis (Supplemental Figure S13). Taking into account the technical caveat of insufficient knockdown, these functional data suggest that additional but limited number of direct FoxO targets participate in control of EC homeostasis as well.

Discussion

In this study, systematic genetic analysis provided the first formal proof that the *FoxO*s are tumor suppressors *in vivo*, albeit with a narrower tumor spectrum than might have been predicted from previous biochemical models but in line with inherited genetic syndromes targeting the PI3K pathway in humans. By demonstrating regulation of distinct sets of putative direct targets by FoxOs in thymocytes and endothelial cells, this study also offers the first molecular insights into the highly tissue-restricted and lineage-specific actions of FoxO *in vivo*.

FoxO transcription factors are functionally redundant in tumor suppression

The requirement for complete deletion of all three FoxO loci in lymphomas, despite mosaic deletion patterns in premalignant thymocytes, combined with the lack of an increased lymphoma incidence in *Mx-Cre*$^{+}$ animals bearing any two floxed alleles, strongly argues for extensive functional redundancy with strong selective pressure for inactivation of all three FoxOs on the level of tumor formation. With regard to the molecular basis of lymphomagenesis in the setting of FoxO deficiency, our *in vitro* studies suggest that increased cell cycle progression as well as resistance to pro-apoptotic stimuli account for the increased incidence of lymphomas *in vivo*. Consistent with this interpretation, $p27^{KIP1}$ (*CDKN1B*), a known T-cell lymphoma suppressor gene (Geisen et al., 2003; Kang-Decker et al., 2004; Martins and Berns, 2002) and FoxO target (Dijkers et al., 2000; Medema et al., 2000; Stahl et al., 2002), was identified as one of the most significantly downregulated genes with a high number of evolutionarily conserved BEs.

It is somewhat unanticipated that the tumour spectrum following deletion of the three FoxOs is so restricted given that misregulation of the PTEN/AKT axis results in a wide range of tumors

including carcinomas (skin, colon, prostate, etc.), which were not observed following deletion of the three FoxOs. It is unlikely that this relates to insufficient *Mx-Cre* activity in epithelial tissue compartments given our documentation of efficient Cre-mediated recombination by PCR and by strong reporter activation in a wide range of epithelial compartments including skin, mammary tissue, and GI tract (Supplemental Figure S8). Furthermore, deletion of the *FoxO*s using K14-Cre, which is strongly expressed in a wide range of epithelia, did not result in epithelial hyperplasia or cancer in animals that were permitted to age normally for up to 16 months of age (D.H.C. and George John, unpublished observations). At the same time, we cannot exclude the possibility that a limited number of epithelial cell types may not be targeted efficiently by *Mx-Cre* and do in fact depend upon FoxO tumor suppression activity, or that certain epithelia require a longer latency than the lethal neoplasias observed in our model. Such considerations gain relevance in light of FoxO1 deletions in a high percentage of human prostate cancers, although the existence of PI3K pathway mutations (e.g., PTEN) remains undetermined in those cancers with FoxO1 alterations (Dong et al., 2006). While the lack of neoplastic phenotypes in epithelial tissues does not diminish the importance of the FoxOs in other cell lineages, our genetic analysis strongly suggests that other signalling surrogates (presumably the mTOR-S6K arm) play more prominent roles in the cancer-relevant activities of the PI3K-AKT network in most epithelial compartments, consistent with the collective data from other labs (Neshat et al., 2001). In this regard, although relatively infrequent, lymphomas have been documented in human *PTEN*-germline syndromes, and alterations in the *PTEN* gene have been reported in spontaneous lymphoid neoplasms (Sakai et al., 1998). Moreover, mice with T cell-specific deletion of *Pten* uniformly develop T cell lymphomas (Suzuki et al., 2001).

In regard to FoxO-deficient vascular phenotype, it is interesting that hemangiomas are characteristic of human disease syndromes resulting from germline *Pten* mutations such as Cowden's disease and Bannayan-Zonana syndrome (Wanner et al., 2001). Thus, demonstration that FoxO inactivation is sufficient to drive development of hemangiomas suggests that misregulation of the FoxOs is a prime mechanism by which PTEN loss leads to hemangiomas in these patients. Along these lines, benign liver hemangiomas associated with TSC2 deficiency display nuclear FoxO due to inactivation of Akt pathway, whereas TSC2 deficiency in a *Pten* $^{+/-}$ background leads to very aggressive lethal hemangiomas wherein FoxOs localize to the cytosol (Manning et al, 2005). Finally, such restricted cancer phenotypes following deletion of all three FoxOs reveals surprisingly tissue-specific roles for PTEN/AKT signalling surrogates in distinct lineages. These observations highlight the value of conducting *in vivo* genetic studies.

The FoxO family regulates endothelial cell homeostasis

Hemangiomas occurred systemically but were most severe in the uterus, perhaps a consequence of the cyclic vascular remodelling that occurs in this organ (Heryanto and Rogers, 2002). Along similar lines, it is tempting to speculate that the hemangioma-susceptible nature of the liver and muscle, but not the pulmonary vasculature, may reflect the remodelling and regenerative capacity of these organ systems in the setting of injury (e.g. hepatectomy) or physiologic stress (e.g. exercise). Much less severe lesions were observed in *Mx-Cre*$^{+}$*;FoxO1*$^{L/L}$ but not in *FoxO3* or *FoxO4* nullizygous mice, arguing that FoxO1 is the most physiologically important regulator of endothelial stability. Nonetheless, successive inactivation of FoxO3 and/or FoxO4 in addition to FoxO1 resulted in hemangioma phenotypes of increasing severity, clearly indicating that both FoxO3 and FoxO4 also contribute to endothelial growth suppression *in vivo*.

Sprouty2 is a major direct target of FoxO in endothelial cells

The rationale for emphasizing Sprouty2 for our in-depth biological validation studies rested on the high number of predicted FoxO DNA BEs, its known functions in branching morphogenesis, and its documented albeit poorly understood roles in growth inhibition. While Sprouty2 is not the sole mediator of the FoxO effects on endothelial cell growth and survival (see below), our studies prove that it is a major effector, as knockdown of Sprouty2 mimicked many of the phenotypic consequences of triple FoxO deletion. The FoxO-Sprouty2 link gains further appeal in light of previous work showing that the Drosophila *Sprouty* homologue functions as an antagonist of receptor tyrosine kinase (RTK) signaling pathways that regulate branching morphogenesis of airways (Hacohen et al., 1998; Kramer et al., 1999), a process with obvious parallels to vasculogenesis. *Sprouty* and its mammalian homologues (*Sprouty1–4*) are general inhibitors of RTK signalling that function by dampening the RAS-RAF-MEK pathway (Gross et al., 2001; Reich et al., 1999). Finally, on a more speculative level, it was recently demonstrated that Sprouty2 protein contains iron-sulfur complexes and assembles into large 24 subunit particles that store electrical charge and thus could serve as intercellular redox sensors (Wu et al., 2005). Furthermore, Sprouty2 is subject to nitrosylation by nitric oxide (NO) (Wu et al., 2005), consistent with studies showing that forced expression of NO synthase phenocopies the *Sprouty* mutation in flies (Wingrove and O'Farrell, 1999). How these provocative findings relate to RTK inhibition remain to be determined, but the link between Sprouty proteins and NO is especially intriguing, given the importance of NO as a regulator of vascular endothelium and response to hypoxia, and the fact that endothelium is a major site of NO synthesis. Thus, many lines of evidence support the view that Sprouty2 is a critical focal point for pathways relevant to vascular biology.

At the same time, despite its potent negative regulatory effect on EC growth and survival, previous analysis of Sprouty2 knockout mice did not show high incidence of hemangioma (Taketomi et al. 2005; Shim et al. 2005). Absence of apparent hemangiomas in Sprouty2 knockout mice may therefore reflect that the FoxO null hemangioma phenotype may require the collaborative impact of additional FoxO target genes. Indeed our functional analysis on an additional set of FoxO-target genes supports this view, pointing to important contributions of PBX1 in FoxO-regulated vascular biology in vivo (Supplemental Figure S13).

In summary, by utilizing the *in vivo* system for somatic deletion of FoxO in multiple cell lineages, which resulted in clear phenotype-genotype correlations, and by employing computational prediction of FoxO binding elements, we obtained evidence that the FoxOs effect unique biological consequences in different cell or tissue contexts via modulation of distinct downstream targets. These observations should motivate further analysis of FoxO targets for the development of novel points of therapeutic intervention in cancer and vascular disease but also emphasize that the proper deployment of such therapies requires a systematic dissection of these targets in specific lineages and the tissue contexts of these lineages.

Experimental Procedures

Targeting constructs, generation, and analysis of mice

See Supplemental Methods.

Immunohistochemistry and immunofluorescence

Formalin-fixed, paraffin-embedded sections were used. For stains of pituitary tumors, sections were incubated with rabbit polyclonal antibodies to prolactin, GH, or ACTH (obtained through NHPP, NIDDK, and Dr. A.F. Parlow) followed by incubation with HRP-goat anti-rabbit IgG (Zymed) or with monoclonal antibodies to TSH, FSH, and LH (LabVision/Neomarkers) utilizing the Histomouse-MAX kit (Zymed). In all cases, sections were then incubated with

DAB and counterstained with hematoxylin. To visualize functional vasculature, we intravenously injected deeply anesthetised mice with 100 μg FITC-labeled tomato lectin (Vector Laboratories) and perfused the hearts with 4% paraformaldehyde; tissues were then frozen in OCT medium. Images were acquired at a 0.5 micron thickness interval using a Zeiss inverted microscope (Axiovert) with automated stage, and image deconvolution was carried out with the nearest neighbor algorithm.

Thymocyte isolation, proliferation, and apoptosis

For analysis of thymocytes, fresh thymus was passed through a cell strainer (Becton Dickinson) in order to produce single cell suspensions for analysis and resuspended in RPMI-1640 media containing 10% fetal calf serum. For thymocyte proliferation assays, cells were seeded in 96-well plates at 1×10^5 cells per well and subjected to the following conditions: no mitogen, PMA (1 ng/ml) + ionomycin (50 ng/ml), and 3 μg/ml anti-CD3e (eBioscience) + 100 U IL-2. Cells were grown for 48 hours, pulsed with 1 μCi [3H]-thymidine (Amersham) for the last 16 hours. Incorporated [3H]-thymidine was measured using the 1450 MicroBeta Trilux Scintillation and Luminescence Counter. For analysis of apoptosis, thymocytes were plated in 12-well plates (1×10^6 cells per well) and treated with 5 Gy gamma-irradiation or 1 μM dexamethasone for 18 hours. Cell viability was determined by staining the cells with propidium iodide and performing flow cytometric analysis.

Flow cytometric analysis

Single cell suspensions of thymus or EC were incubated with the following monoclonal antibodies: anti-CD4 (PE- or FITC-conjugated), anti-CD8 (PE- or APC-conjugated), anti-Mac-1-FITC, anti-CD3-PE, anti-CD25-APC, anti-CD44-PE, anti-Gr-1-PE, anti-CD19-APC, and anti-CD31-FITC (all from PharMingen). Flow cytometry analysis was performed on freshly stained samples.

Isolation and characterization of endothelial cells, microarray analysis and FoxO DNA binding element studies

See supplemental methods.

Quantitative real-time PCR analysis

RNA was harvested using Trizol (Invitrogen) and the RNeasy kit (Qiagen). RNA was treated with RQ1 RNase-freeDNase (Promega), and cDNA was prepared utilizing Superscript II Rnase H-Reverse transcriptase (Invitrogen). Quantitative real-time PCR was performed on cDNA samples utilizing the Quantitect SYBR Green PCR kit (Qiagen) and was run on the Stratagene Mx3000P. Primer sequences are available upon request.

Western blot analysis

Tissues and cells were lysed with RIPA buffer (20 mM Tris pH 7.5, 150 mM NaCl, 1% Nonidet P-40, 0.5% Sodium Deoxycholate, 1 mM EDTA, 0.1% SDS) containing complete mini protease inhibitors (Roche). Western blots were performed utilizing 50 μg of lysate protein, incubated with the following antibodies: anti-FKHR(FoxO1)/AFX(FoxO4) (Cell Signaling Technology) and anti-FKHRL1(FoxO3) (Upstate Biotechnology).

Supplementary Material

Refer to Web version on PubMed Central for supplementary material.

Acknowledgements

We are grateful Sarah Weiler and Mychelle Neptune for the generation of the conditional FoxO knockout mouse strains. We are also grateful to Karen Marmon, Alice Yu, and Yan Zhang for their assistance in the animal facility. We thank Nabeel El-Bardeesy, Susan Dymecki, Klaus Rajewsky, A.F. Parlow, the NCI BRB Preclinical Repository for reagents, and the DFCI-Broad RNAi Consortium for lentiviral shRNA vectors. We also thank Dong-In Yuk for assistance with RISH. D.G.G. is an Investigator of the Howard Hughes Medical Institute. J-H.P. and Z.D. are Damon Runyon Fellows supported by the Damon Runyon Cancer Research Foundation. D.H.C. is a Sidney Kimmel Foundation Scholar and supported by the Mary Kay Ash and Lance Armstrong Foundations. This work was supported by grants to D.H.C., D.G.G., L.C., W.H.W., and R.A.D. from the NIH. R.A.D. is an American Cancer Society Research Professor and an Ellison Medical Foundation Scholar and supported by the Robert A. and Renee E. Belfer Foundation Institute for Innovative Cancer Science.

References

Anderson MJ, Viars CS, Czekay S, Cavenee WK, Arden KC. Cloning and characterization of three human forkhead genes that comprise an FKHR-like gene subfamily. Genomics 1998;47:187–199. [PubMed: 9479491]

Benezra R. Role of Id proteins in embryonic and tumor angiogenesis. Trends Cardiovasc Med 2001;11:237–241. [PubMed: 11673054]

Biggs WH 3rd, Cavenee WK, Arden KC. Identification and characterization of members of the FKHR (FOX O) subclass of winged-helix transcription factors in the mouse. Mamm Genome 2001;12:416–425. [PubMed: 11353388]

Bikfalvi A, Klein S, Pintucci G, Rifkin DB. Biological roles of fibroblast growth factor-2. Endocr Rev 1997;18:26–45. [PubMed: 9034785]

Brunet A, Bonni A, Zigmond MJ, Lin MZ, Juo P, Hu LS, Anderson MJ, Arden KC, Blenis J, Greenberg ME. Akt promotes cell survival by phosphorylating and inhibiting a Forkhead transcription factor. Cell 1999;96:857–868. [PubMed: 10102273]

Castrillon DH, Miao L, Kollipara R, Horner JW, DePinho RA. Suppression of ovarian follicle activation in mice by the transcription factor Foxo3a. Science 2003;301:215–218. [PubMed: 12855809]

Cook-Mills JM. VCAM-1 signals during lymphocyte migration: role of reactive oxygen species. Mol Immunol 2002;39:499–508. [PubMed: 12431382]

Cross DA, Alessi DR, Cohen P, Andjelkovich M, Hemmings BA. Inhibition of glycogen synthase kinase-3 by insulin mediated by protein kinase B. Nature 1995;378:785–789. [PubMed: 8524413]

Cully M, You H, Levine AJ, Mak TW. Beyond PTEN mutations: the PI3K pathway as an integrator of multiple inputs during tumorigenesis. Nat Rev Cancer 2006;6:184–192. [PubMed: 16453012]

Di Cristofano A, Pesce B, Cordon-Cardo C, Pandolfi PP. Pten is essential for embryonic development and tumour suppression. Nat Genet 1998;19:348–355. [PubMed: 9697695]

Dijkers PF, Medema RH, Pals C, Banerji L, Thomas NS, Lam EW, Burgering BM, Raaijmakers JA, Lammers JW, Koenderman L, et al. Forkhead transcription factor FKHR-L1 modulates cytokine-dependent transcriptional regulation of p27(KIP1). Mol Cell Biol 2000;20:9138–9148. [PubMed: 11094066]

Dong XY, Chen C, Sun X, Guo P, Vessella RL, Wang RX, Chung LW, Zhou W, Dong JT. FOXO1A is a candidate for the 13q14 tumor suppressor gene inhibiting androgen receptor signaling in prostate cancer. Cancer research 2006;66:6998–7006. [PubMed: 16849544]

Ferrara N, Gerber HP, LeCouter J. The biology of VEGF and its receptors. Nat Med 2003;9:669–676. [PubMed: 12778165]

Flores ER, Sengupta S, Miller JB, Newman JJ, Bronson R, Crowley D, Yang A, McKeon F, Jacks T. Tumor predisposition in mice mutant for p63 and p73: evidence for broader tumor suppressor functions for the p53 family. Cancer cell 2005;7:363–373. [PubMed: 15837625]

Flores ER, Tsai KY, Crowley D, Sengupta S, Yang A, McKeon F, Jacks T. p63 and p73 are required for p53-dependent apoptosis in response to DNA damage. Nature 2002;416:560–564. [PubMed: 11932750]

Freeman D, Lesche R, Kertesz N, Wang S, Li G, Gao J, Groszer M, Martinez-Diaz H, Rozengurt N, Thomas G, et al. Genetic background controls tumor development in PTEN-deficient mice. Cancer research 2006;66:6492–6496. [PubMed: 16818619]

Furuyama T, Kitayama K, Shimoda Y, Ogawa M, Sone K, Yoshida-Araki K, Hisatsune H, Nishikawa S, Nakayama K, Ikeda K, et al. Abnormal angiogenesis in Foxo1 (Fkhr)-deficient mice. The Journal of biological chemistry 2004;279:34741–34749. [PubMed: 15184386]

Furuyama T, Nakazawa T, Nakano I, Mori N. Identification of the differential distribution patterns of mRNAs and consensus binding sequences for mouse DAF-16 homologues. Biochem J 2000;349:629–634. [PubMed: 10880363]

Geisen C, Karsunky H, Yucel R, Moroy T. Loss of p27(Kip1) cooperates with cyclin E in T-cell lymphomagenesis. Oncogene 2003;22:1724–1729. [PubMed: 12642875]

Goumans MJ, Lebrin F, Valdimarsdottir G. Controlling the angiogenic switch: a balance between two distinct TGF-b receptor signaling pathways. Trends Cardiovasc Med 2003;13:301–307. [PubMed: 14522471]

Gross I, Bassit B, Benezra M, Licht JD. Mammalian sprouty proteins inhibit cell growth and differentiation by preventing ras activation. The Journal of biological chemistry 2001;276:46460–46468. [PubMed: 11585837]

Hacohen N, Kramer S, Sutherland D, Hiromi Y, Krasnow MA. sprouty encodes a novel antagonist of FGF signaling that patterns apical branching of the Drosophila airways. Cell 1998;92:253–263. [PubMed: 9458049]

Hay N. The Akt-mTOR tango and its relevance to cancer. Cancer cell 2005;8:179–183. [PubMed: 16169463]

Hayashi M, Kim SW, Imanaka-Yoshida K, Yoshida T, Abel ED, Eliceiri B, Yang Y, Ulevitch RJ, Lee JD. Targeted deletion of BMK1/ERK5 in adult mice perturbs vascular integrity and leads to endothelial failure. J Clin Invest 2004;113:1138–1148. [PubMed: 15085193]

Heryanto B, Rogers PA. Regulation of endometrial endothelial cell proliferation by oestrogen and progesterone in the ovariectomized mouse. Reproduction 2002;123:107–113. [PubMed: 11869192]

Hosaka T, Biggs WH 3rd, Tieu D, Boyer AD, Varki NM, Cavenee WK, Arden KC. Disruption of forkhead transcription factor (FOXO) family members in mice reveals their functional diversification. Proc Natl Acad Sci U S A 2004;101:2975–2980. [PubMed: 14978268]

Inoki K, Li Y, Zhu T, Wu J, Guan KL. TSC2 is phosphorylated and inhibited by Akt and suppresses mTOR signalling. Nat Cell Biol 2002;4:648–657. [PubMed: 12172553]

Jacobs FM, van der Heide LP, Wijchers PJ, Burbach JP, Hoekman MF, Smidt MP. FoxO6, a novel member of the FoxO class of transcription factors with distinct shuttling dynamics. The Journal of biological chemistry 2003;278:35959–35967. [PubMed: 12857750]

Junger MA, Rintelen F, Stocker H, Wasserman JD, Vegh M, Radimerski T, Greenberg ME, Hafen E. The Drosophila forkhead transcription factor FOXO mediates the reduction in cell number associated with reduced insulin signaling. J Biol 2003;2:20. [PubMed: 12908874]

Kang-Decker N, Tong C, Boussouar F, Baker DJ, Xu W, Leontovich AA, Taylor WR, Brindle PK, van Deursen JM. Loss of CBP causes T cell lymphomagenesis in synergy with p27Kip1 insufficiency. Cancer cell 2004;5:177–189. [PubMed: 14998493]

Kato J, Tsuruda T, Kita T, Kitamura K, Eto T. Adrenomedullin: a protective factor for blood vessels. Arterioscler Thromb Vasc Biol 2005;25:2480–2487. [PubMed: 16141406]

Kramer S, Okabe M, Hacohen N, Krasnow MA, Hiromi Y. Sprouty: a common antagonist of FGF and EGF signaling pathways in Drosophila. Development 1999;126:2515–2525. [PubMed: 10226010]

Kuhn R, Schwenk F, Aguet M, Rajewsky K. Inducible gene targeting in mice. Science 1995;269:1427–1429. [PubMed: 7660125]

Le Jan S, Amy C, Cazes A, Monnot C, Lamande N, Favier J, Philippe J, Sibony M, Gasc JM, Corvol P, et al. Angiopoietin-like 4 is a proangiogenic factor produced during ischemia and in conventional renal cell carcinoma. Am J Pathol 2003;162:1521–1528. [PubMed: 12707035]

Lee MH, Williams BO, Mulligan G, Mukai S, Bronson RT, Dyson N, Harlow E, Jacks T. Targeted disruption of p107: functional overlap between p107 and Rb. Genes Dev 1996;10:1621–1632. [PubMed: 8682293]

Li G, Robinson GW, Lesche R, Martinez-Diaz H, Jiang Z, Rozengurt N, Wagner KU, Wu DC, Lane TF, Liu X, et al. Conditional loss of PTEN leads to precocious development and neoplasia in the mammary gland. Development 2002;129:4159–4170. [PubMed: 12163417]

Lin L, Hron JD, Peng SL. Regulation of NF-kappaB, Th activation, and autoinflammation by the forkhead transcription factor Foxo3a. Immunity 2004;21:203–213. [PubMed: 15308101]

Martins CP, Berns A. Loss of p27(Kip1) but not p21(Cip1) decreases survival and synergizes with MYC in murine lymphomagenesis. Embo J 2002;21:3739–3748. [PubMed: 12110586]

Medema RH, Kops GJ, Bos JL, Burgering BM. AFX-like Forkhead transcription factors mediate cell-cycle regulation by Ras and PKB through p27kip1. Nature 2000;404:782–787. [PubMed: 10783894]

Mouta Carreira C, Nasser SM, di Tomaso E, Padera TP, Boucher Y, Tomarev SI, Jain RK. LYVE-1 is not restricted to the lymph vessels: expression in normal liver blood sinusoids and down-regulation in human liver cancer and cirrhosis. Cancer research 2001;61:8079–8084. [PubMed: 11719431]

Neshat MS, Mellinghoff IK, Tran C, Stiles B, Thomas G, Petersen R, Frost P, Gibbons JJ, Wu H, Sawyers CL. Enhanced sensitivity of PTEN-deficient tumors to inhibition of FRAP/mTOR. Proc Natl Acad Sci U S A 2001;98:10314–10319. [PubMed: 11504908]

Nikitenko LL, Fox SB, Kehoe S, Rees MC, Bicknell R. Adrenomedullin and tumour angiogenesis. Br J Cancer 2006;94:1–7. [PubMed: 16251875]

Podsypanina K, Ellenson LH, Nemes A, Gu J, Tamura M, Yamada KM, Cordon-Cardo C, Catoretti G, Fisher PE, Parsons R. Mutation of Pten/Mmac1 in mice causes neoplasia in multiple organ systems. Proc Natl Acad Sci U S A 1999;96:1563–1568. [PubMed: 9990064]

Potente M, Urbich C, Sasaki KI, Hofmann WK, Heeschen C, Aicher A, Kollipara R, Depinho RA, Zeiher AM, Dimmeler S. Involvement of Foxo transcription factors in angiogenesis and postnatal neovascularization. J Clin Invest. 2005

Puig O, Marr MT, Ruhf ML, Tjian R. Control of cell number by Drosophila FOXO: downstream and feedback regulation of the insulin receptor pathway. Genes Dev 2003;17:2006–2020. [PubMed: 12893776]

Ramirez F, Pereira L, Zhang H, Lee B. The fibrillin-Marfan syndrome connection. Bioessays 1993;15:589–594. [PubMed: 8240311]

Reich A, Sapir A, Shilo B. Sprouty is a general inhibitor of receptor tyrosine kinase signaling. Development 1999;126:4139–4147. [PubMed: 10457022]

Sage J, Mulligan GJ, Attardi LD, Miller A, Chen S, Williams B, Theodorou E, Jacks T. Targeted disruption of the three Rb-related genes leads to loss of G(1) control and immortalization. Genes Dev 2000;14:3037–3050. [PubMed: 11114892]

Schneider A, Zhang Y, Guan Y, Davis LS, Breyer MD. Differential, inducible gene targeting in renal epithelia, vascular endothelium, and viscera of Mx1Cre mice. Am J Physiol Renal Physiol 2003;284:F411–417. [PubMed: 12529277]

Seoane J, Le HV, Shen L, Anderson SA, Massague J. Integration of Smad and forkhead pathways in the control of neuroepithelial and glioblastoma cell proliferation. Cell 2004;117:211–223. [PubMed: 15084259]

Shiojima I, Walsh K. Role of Akt signaling in vascular homeostasis and angiogenesis. Circ Res 2002;90:1243–1250. [PubMed: 12089061]

Skurk C, Maatz H, Kim HS, Yang J, Abid MR, Aird WC, Walsh K. The Akt-regulated forkhead transcription factor FOXO3a controls endothelial cell viability through modulation of the caspase-8 inhibitor FLIP. The Journal of biological chemistry 2004;279:1513–1525. [PubMed: 14551207]

Stahl M, Dijkers PF, Kops GJ, Lens SM, Coffer PJ, Burgering BM, Medema RH. The forkhead transcription factor FoxO regulates transcription of p27Kip1 and Bim in response to IL-2. J Immunol 2002;168:5024–5031. [PubMed: 11994454]

Suzuki A, Yamaguchi MT, Ohteki T, Sasaki T, Kaisho T, Kimura Y, Yoshida R, Wakeham A, Higuchi T, Fukumoto M, et al. T cell-specific loss of Pten leads to defects in central and peripheral tolerance. Immunity 2001;14:523–534. [PubMed: 11371355]

van der Heide LP, Jacobs FM, Burbach JP, Hoekman MM, Smidt MP. FoxO6 transcriptional activity is regulated by Thr26 and Ser184, independent of nucleo-cytoplasmic shuttling. Biochem J. 2005

Wang S, Gao J, Lei Q, Rozengurt N, Pritchard C, Jiao J, Thomas GV, Li G, Roy-Burman P, Nelson PS, et al. Prostate-specific deletion of the murine Pten tumor suppressor gene leads to metastatic prostate cancer. Cancer cell 2003;4:209–221. [PubMed: 14522255]

Wanner M, Celebi JT, Peacocke M. Identification of a PTEN mutation in a family with Cowden syndrome and Bannayan-Zonana syndrome. J Am Acad Dermatol 2001;44:183–187. [PubMed: 11174374]

Wingrove JA, O'Farrell PH. Nitric oxide contributes to behavioral, cellular, and developmental responses to low oxygen in Drosophila. Cell 1999;98:105–114. [PubMed: 10412985]

Wu X, Alexander PB, He Y, Kikkawa M, Vogel PD, McKnight SL. Mammalian sprouty proteins assemble into large monodisperse particles having the properties of intracellular nanobatteries. Proc Natl Acad Sci U S A 2005;102:14058–14062. [PubMed: 16172380]

You MJ, Castrillon DH, Bastian BC, O'Hagan RC, Bosenberg MW, Parsons R, Chin L, DePinho RA. Genetic analysis of Pten and Ink4a/Arf interactions in the suppression of tumorigenesis in mice. Proc Natl Acad Sci U S A 2002;99:1455–1460. [PubMed: 11818530]

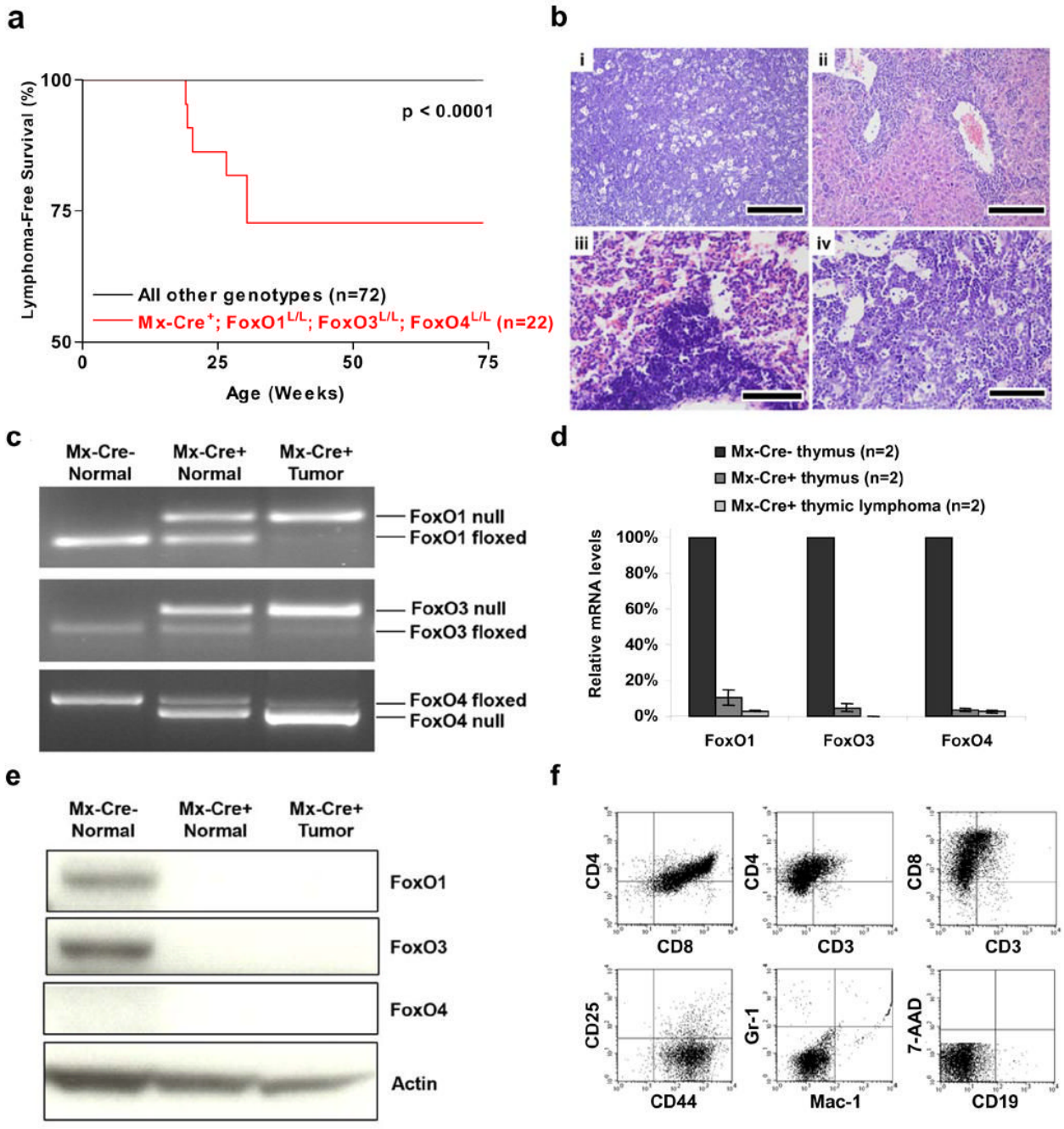

Figure 1. Thymic lymphomas in mice following somatic deletion of three *FoxO* genes

a, Thymic lymphoma-free survival of pI-pC treated *Mx-Cre*$^{+}$ mice and controls representing combined genotypes including: *Mx-Cre*$^{+}$*;FoxO1*$^{L/L}$ (n=11), *Mx-Cre*$^{+}$*;FoxO1/3*$^{L/L}$ (n=14), *Mx-Cre*$^{+}$*;FoxO1/4*$^{L/L}$ (n=11), and all *Mx-Cre*$^{-}$ controls (n=36). No lymphomas were observed in controls up to 100 weeks of age. **b**, Histology and tissue infiltration of thymic lymphoma in *Mx-Cre*$^{+}$ mouse, H&E stains. (i) thymus (ii) liver, (iii) lung, and (iv) bone marrow. Scale bars: 200 μm (i and ii) and 100 μm (iii and iv). **c**, *FoxO1*, *FoxO3*, and *FoxO4* gene deletions in thymic lymphomas and control thymi by PCR analysis. **d**, Reduction of mRNA levels of *FoxO1*, *FoxO3*, and *FoxO4* in *Mx-Cre*$^{+}$ endothelial cells. Quantitative real-time PCR performed on *Mx-Cre*$^{-}$ thymi (7 weeks), *Mx-Cre*$^{+}$ thymi (7 weeks), and *Mx-Cre*$^{+}$ thymic

lymphomas (n=2, 19 and 30 weeks post pI-pC); relative reduction of *FoxO* levels relative to *Mx-Cre*$^{-}$ thymi is shown. **e**, Western blot analysis of *Mx-Cre*$^{-}$ and *Mx-Cre*$^{+}$ thymi and thymic lymphoma samples. **f**, Flow cytometric analysis of representative thymic lymphoma.

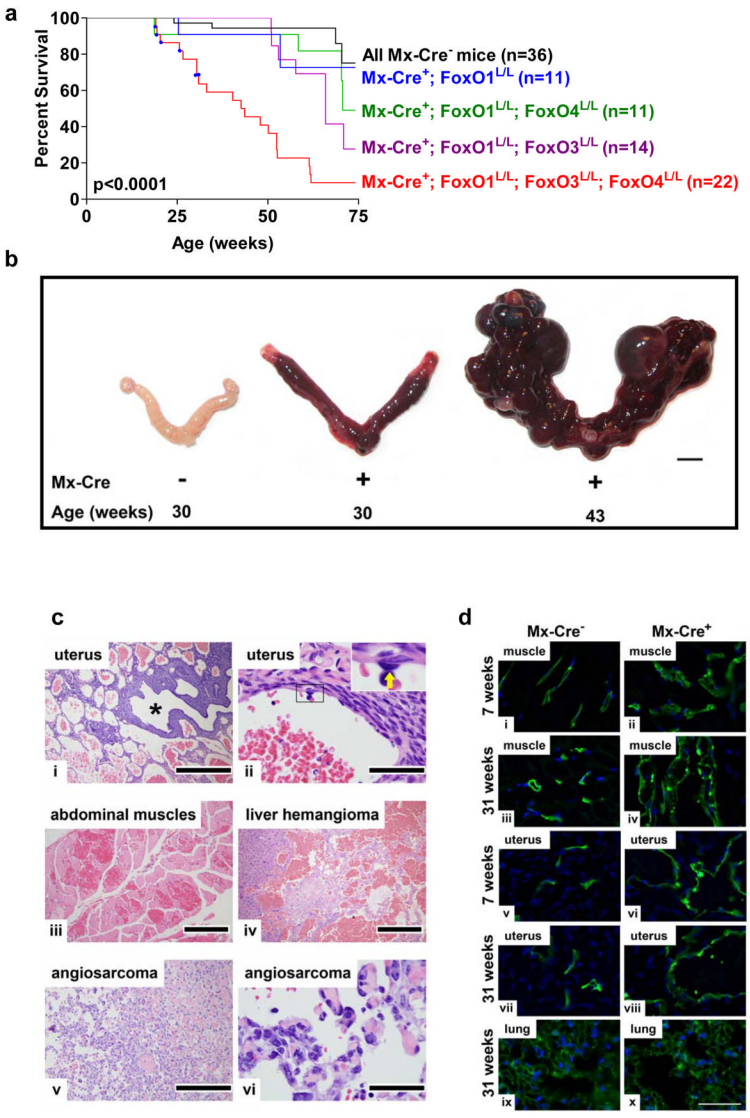

Figure 2. Systemic hemangiomas in mice following somatic deletion of three *FoxO* alleles

a, Survival of *Mx-Cre*$^{+}$ and *Mx-Cre*$^{-}$ littermates controls. Blue squares indicate deaths due to thymic lymphomas. P value indicates comparison between *Mx-Cre*$^{+}$ mice (red) and all *Mx-Cre*$^{-}$ controls (black). **b**, Age-dependent progression of uterine vascular lesions in *Mx-Cre*$^{+}$ females, scale Bar=5 mm. **c**, Histology of systemic vascular lesions, H&E stains. Genotypes are *Mx-Cre*$^{+}$ unless otherwise noted. i, uterus, low magnification (asterisk: uterine lumen); ii, uterine hemangioma (inset: benign endothelium of hemangioma vascular channels; arrow: endothelial cell); iii, abdominal muscle hemangioma; iv, liver hemangioma, *Mx-Cre*$^{+}$ mouse; v-vi, angiosarcoma, *Mx-Cre*$^{+}$ mouse. Scale bars: 500 μm (i and v), 400 μm (iv), 200 μm (iii), and 50 μm (ii and vi). **d,** Fluorescence micrographs of abdominal muscle, uterine horn, and lung endothelium after vascular perfusion of fluorescein-labeled lectin (blue: DAPI labelled nuclei). Note increased endothelial cell density by 7 weeks in muscle and uterine horn but not in lung as late as 31 weeks. Scale bar=50 μm.

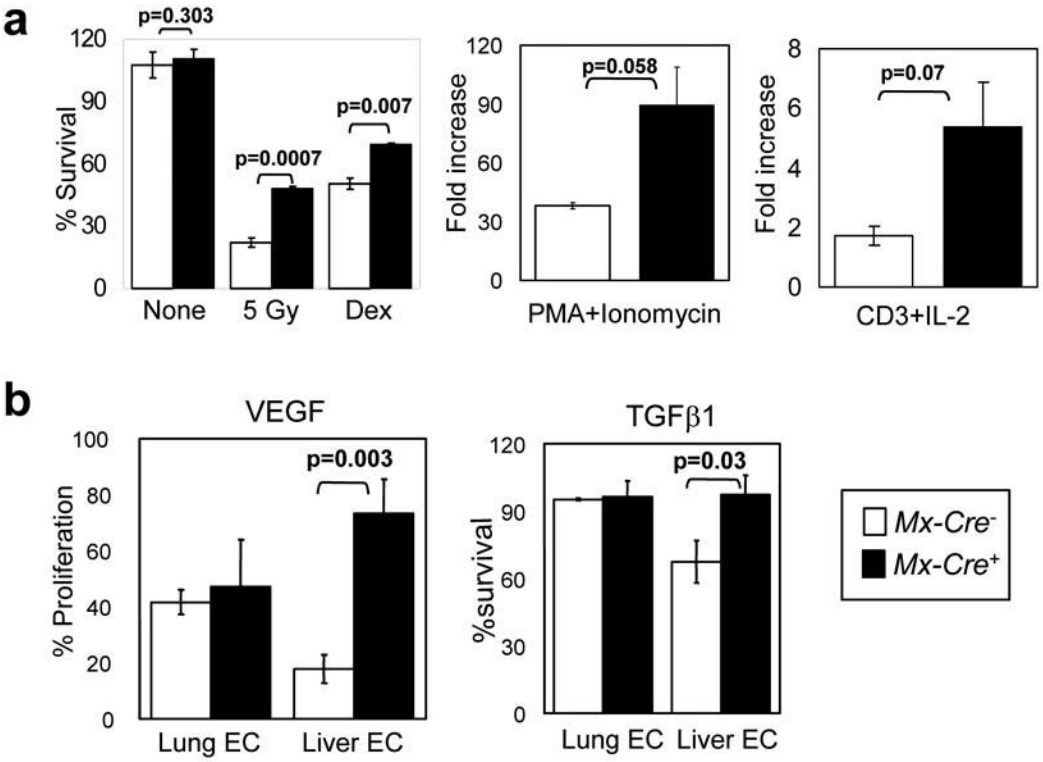

Figure 3. Functional studies of thymocytes and endothelial cells rendered null for all three *FoxOs*

a, Increased proliferation and defective induction of apoptosis in *Mx-Cre*$^{+}$ thymocytes. Thymocytes from 8-week old mice (n=3 per genotype) were plated and the indicated mitogens or apoptotic stimuli were applied. Experiment was performed twice with similar results; data from a representative experiment is shown. Survival % was calculated after 18hrs of treatment (5 Gy: γ-irradiation; Dex: 1 μM Dexamethasone). **b**, Analysis of viability of endothelial cells. MTT assays were performed on *Mx-Cre*$^{-}$ and *Mx-Cre*$^{+}$ lung (n=2) and liver (n=3) ECs. Y axis, normalized response (%) per OD595. Results represent two independent experiments. For a and b, data are mean ± SEM.

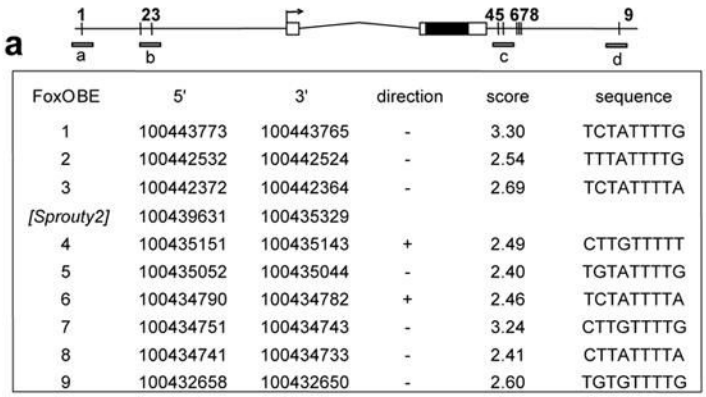

FoxOBE	5'	3'	direction	score	sequence
1	100443773	100443765	-	3.30	TCTATTTTG
2	100442532	100442524	-	2.54	TTTATTTTG
3	100442372	100442364	-	2.69	TCTATTTTA
[Sprouty2]	100439631	100435329			
4	100435151	100435143	+	2.49	CTTGTTTTT
5	100435052	100435044	-	2.40	TGTATTTTG
6	100434790	100434782	+	2.46	TCTATTTTA
7	100434751	100434743	-	3.24	CTTGTTTTG
8	100434741	100434733	-	2.41	CTTATTTTA
9	100432658	100432650	-	2.60	TGTGTTTTG

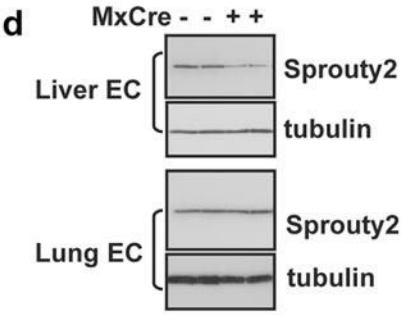

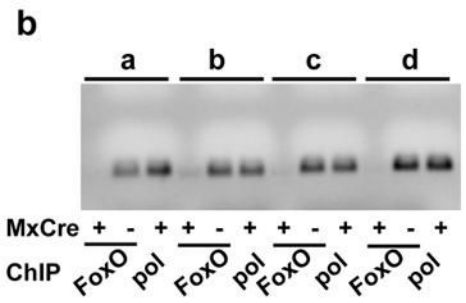

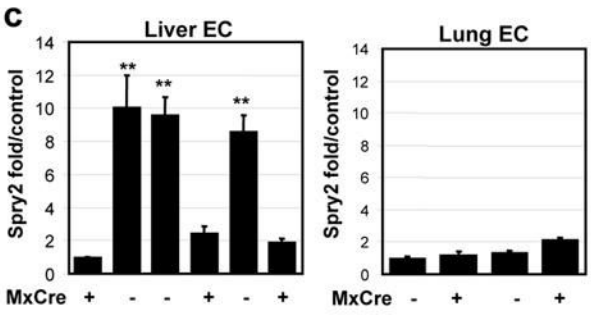

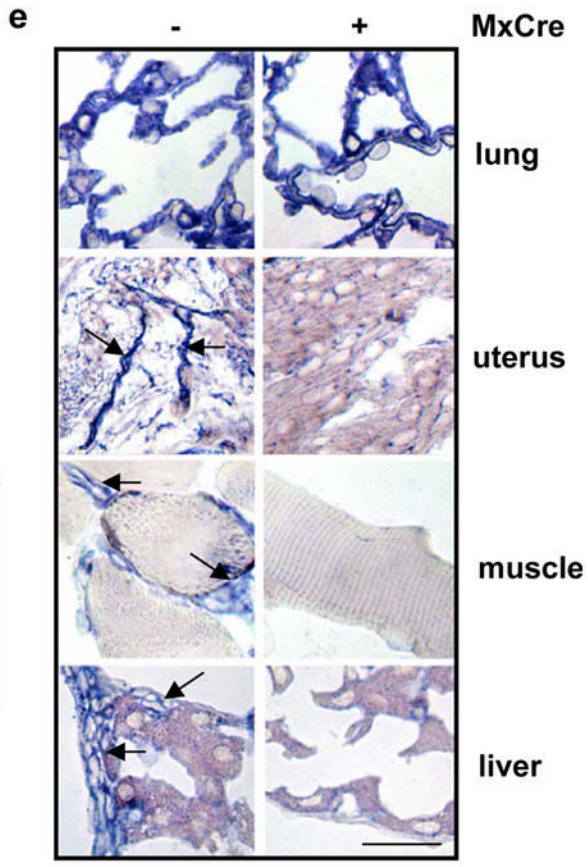

Figure 4. Regulation of Sprouty2 expression in liver ECs by FoxOs

a, Multiple conserved FoxO binding sites (predicted) in vicinity of *Sprouty2* gene; ~11kb of the genomic region is shown. 5 of 10 sites were conserved in >3 species including human and mouse (supplementary methods). Sites were scored by 10-based logarithm of the likelihood ratio between the FoxO and background models. **b.** The FoxO BE occupancy by FoxOs. Soluble chromatin was prepared from *Mx-Cre*$^{-}$ and *Mx- Cre*$^{+}$ liver ECs and immunoprecipitated with a mixture of antibodies against the 3 FoxOs. Anti-pol II and anti-FoxO immunoprecipitated DNA (FoxO) was amplified giving rise to ~110bp products (a-d, illustrated in panel **a). c**, Quantitative real-time PCR analysis for Sprouty2. Expression of Sprouty2 is tightly correlated with FoxO deletion (*Mx-Cre*$^{+}$*)* in liver ECs but not in lung ECs (**, $p<0.01$); error bars = s.e. **d**. Immunoblot analysis for Sprouty2. Expression of Sprouty2

is lower in FoxO deletion (*Mx-Cre*$^{+}$*)* in liver ECs but not in lung ECs compared with control ECs. Duplicate loading shown for each EC line. **e.** RNA in situ hybridization using antisense Sprouty2 probe tissues from *Mx-Cre*$^{-}$ and *Mx-Cre*$^{+}$ mice 3 weeks after pI-pC injection. Arrows point to EC with strong Sprouty2 expression (bar=20μm).

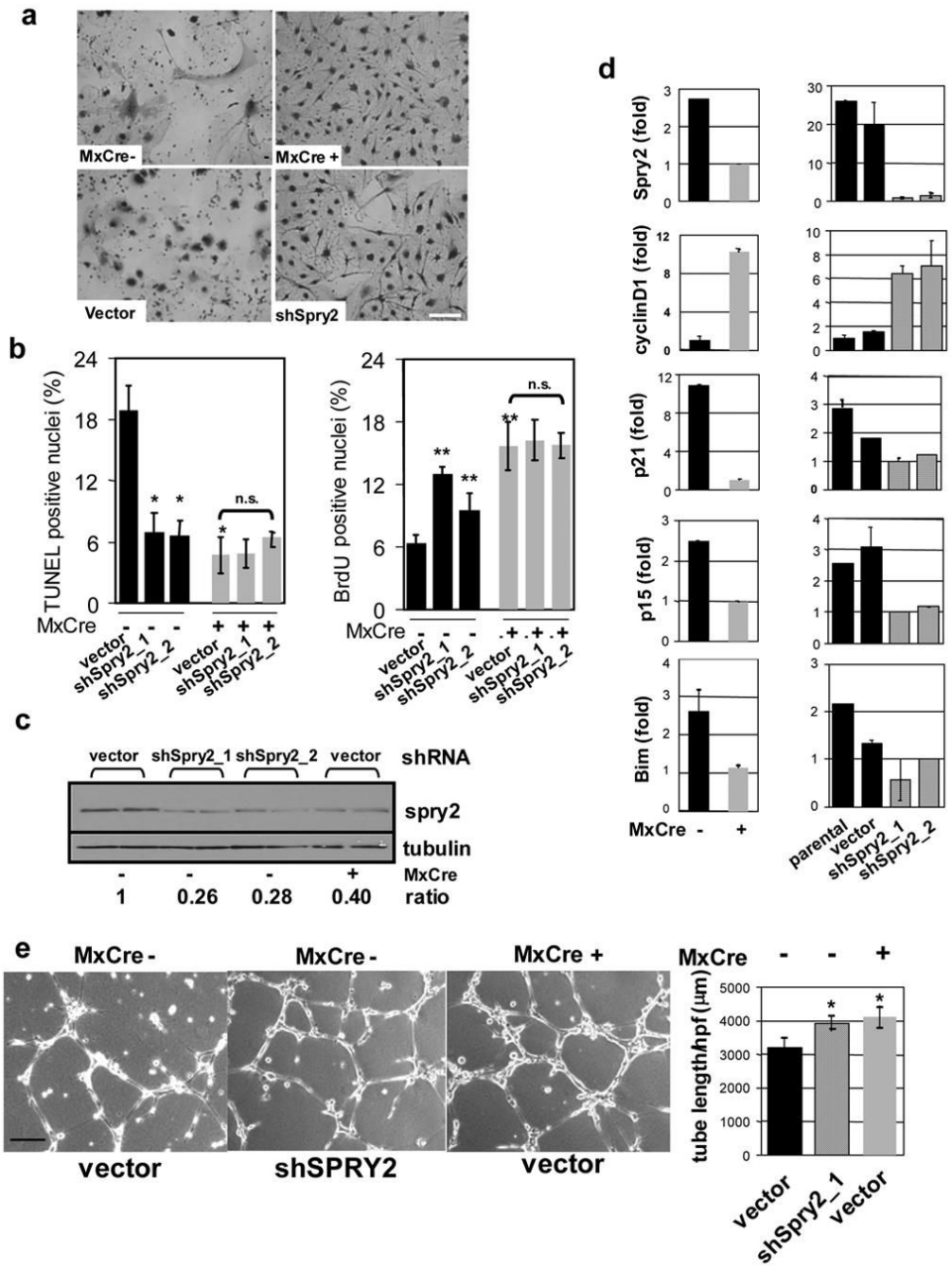

Figure 5. FoxOs regulate liver EC angiogenic response through Sprouty2

a, Growth advantage of *Mx-Cre*$^{+}$over *Mx-Cre*$^{-}$ liver ECs after 10 days culture. Sprouty2 knockdown in *Mx-Cre*$^{-}$ liver ECs had similar effect. Bar=15μm. **b**, TUNEL and BrdU. Knockdown of Sprouty2 (shSpry2_1 &_2, shRNAs) in *Mx-Cre*$^{-}$ liver ECs phenocopies cell growth and apoptosis phenotypes in *Mx-Cre*$^{+}$ liver ECs; * indicates $p<0.01$; error bars represent ± s.e. **c,** knock-down of endogenous Sprouty2 protein expression in *Mx-Cre*$^{-}$ liver ECs by shSpry2. Two independent replicates are shown. Band densities were measured by ImageJ and normalized to tubulin. Ratio indicates normalized values over that of control (vector infected *Mx-Cre*$^{-}$ EC). **d**, Correlation of Sprouty2 expression with cyclinD1, p21, p15, Bim level in liver ECs by quantitative PCR analysis. Knockdown of Sprouty2 with two different shRNAs

(shSpry2_1 &_2) recapitulates above differences for cyclinD1, p21, p15, and Bim relative to parental untreated and vector-only controls (lower panels). Results shown are from triplicate experiments; error bars represent ± s.e. **e,** VEGF-induced tube formation in liver ECs. Bar=100 μm. Average tubule length/HPF (±s.d.) measured by ImageJ software in multiple microscopic fields was plotted (*, $p<0.01$ versus vector infected *Mx-Cre*$^{-}$ EC).

Table 1

FoxO targets in liver EC

	# of BE(s)	Conservation Score	# of 3-species BE(s)	CIS	validated by RT-qPCR	validated by ChIP	validated by ISH
Downregulated FoxO Target Genes							
Spry2	10	28	5		YES	YES	YES
Tcf4	10	27	4		YES	nd	YES
Klf6	10	28	3		YES	nd	NO
Cited2	6	17	2		YES	YES	YES
Adm	5	15	2		YES	YES	YES
Ccrn4l	4	12	1		YES	YES	YES
Hmga2	1	3	1		nd	nd	nd
Mrc1	1	3	1		YES	YES	nd
Ctgf	1	3	1		YES	YES	YES
Upregulated FoxO Target Genes							
Meis1	10	28	4	Evi8	YES	nd	NO
Pbx1	11	32	3		YES	YES	YES
Tsc22d1	3	9	2		YES	nd	YES
Ccnd1	8	25	1	Ccnd1	YES	nd	nd
Sdpr	4	11	1		YES	nd	YES
Sepm	4	12	1		nd	nd	nd
Fbn1	4	12	1		YES	nd	YES
Bmper	4	12	1		YES	YES	YES
Rab34	3	9	1		YES	nd	nd
D0H4S114	3	9	1		nd	nd	nd
Pcolce	2	6	1		nd	nd	nd
Id1	1	3	1		YES	nd	YES

YES: validated

NO ; non-validated

nd: not determined

Table 2

FoxO targets in thymocyte

	# of BE(s)	Conservation Score	# of 3-species BE (s)	CIS		# of BE(s)	Conservation Score	# of 3-species BE (s)	CIS
Downregulated FoxO Target Genes					**Upregulated FoxO Target Genes**				
Npas3	10	29	6		Sox5	25	71	6	Btl27
Cdh8	10	31	4		Rora	14	39	4	
Myef2	6	16	3		Cacna2d1	13	37	3	
Cdkn1b	5	14	3		Creb5	11	31	3	
Dlgap1	10	29	2	Btl14	Igsf4d	11	32	3	
Tmem25	8	23	2		Srgap3	10	29	3	
Lrrtm3	7	20	2		Pfkfb2	7	19	3	
Tbx4	5	14	2		Pacs1	6	17	3	
Kcnj2	5	16	2		Sox4	5	14	3	Evi16
AJ430384	4	12	2		Mmp16	11	33	2	
Efna5	4	12	2		Slc12a1	9	25	2	
Rest	8	22	1		Dcamkl1	6	17	2	
Odz3	7	19	1		4931406I20Rik	6	17	2	4931406I20Rik
Dpf3	5	15	1		Scn5a	5	15	2	
Bag5	5	13	1		Sorl1	4	12	2	
Cacna1e	4	11	1		Pou4f3	4	11	2	
Olfm3	3	9	1		Shox2	11	32	1	
Gas7	3	9	1		Hoxd12	6	19	1	
Tmem71	3	9	1		Id4	6	17	1	
Znrf4	3	8	1		Hapln1	6	17	1	
Aqp7	2	6	1		Slc12a1	5	14	1	
C730036D15Rik	2	6	1		Golph4	5	14	1	
Kcnip4	2	6	1		Slc24a2	5	15	1	
Usp3	2	6	1	Evi98	Ppp1r9a	5	15	1	
Myo1e	2	6	1		Barx2	5	15	1	
Tgfbr2	2	6	1		Ddx47	4	11	1	
Cdh23	2	6	1		Abcd2	4	12	1	
Trem2	2	6	1		Npy2r	3	9	1	
Klc3	1	3	1		Shrm	3	8	1	
Cryab	1	3	1		Igfbp3	3	8	1	
Cacna2d2	1	3	1		Flt1	2	6	1	
Ncbp2	1	3	1		Dyx1c1	2	5	1	
Dmrt3	1	3	1		D14Ertd171e	2	5	1	